Asian Journal of Chemistry; Vol. 38, No. 4 (2026), 956-962
ASIAN JOURNAL OF CHEMISTRY
https://doi.org/10.14233/ajchem.2026.35478

Pyrimidine-Piperazine Hybrids as Potential PARP1 Inhibitors: Dual *in silico* and *in vitro* Approaches against Breast Cancer

RASHMI SHIVAKUMAR[1], NARASIMHA M. BEERAKA[2,3], TORESHETTAHALLY R. SWAROOP[1], ZHANG XI[4], D.C. VINAY KUMAR[5], SYED HIDAYATHULLA[6] and BASAPPA BASAPPA[1,*]

[1]Department of Studies in Organic Chemistry, University of Mysore, Manasagangotri, Mysuru-570006, India
[2]Department of Human Anatomy and Histology, I. M. Sechenov First Moscow State Medical University of the Ministry of Health of the Russian Federation (Sechenov University), 8/2 Trubetskaya Str., Moscow 119991, Russia
[3]Saveetha Institute of Basic Medical Sciences (SIBMS), Saveetha Institute of Medical and Technical Sciences, Saveetha University, Chennai-600077, India
[4]Shenzhen Bay Laboratory, Shenzhen-518055, P.R. China
[5]Department of Physics, The National Institute of Engineering North Campus, Mysuru-570008, India
[6]Department of Studies in Molecular Biology, University of Mysore, Mysuru-570006, India

*Corresponding author: E-mail: salundibasappa@gmail.com

Received: 17 December 2025 *Accepted*: 10 February 2026 *Published online*: 8 April 2026 AJC-22316

Pyrimidine derivatives are known to possess notable anticancer properties. In this study, a new series of pyrimidine-piperazine hybrid compounds (**8a-j**) was synthesised and evaluated for cytotoxic and PARP1 inhibitory activities against MCF-7 breast cancer cells. The IC_{50} values against this cell line were determined by Alamar blue assay. The poly(ADP-ribose) polymerase-1 (PARP1) catalytic activity was assessed through a fluorescence-based enzymatic assay. Among the synthesised compounds, **8e** demonstrated the highest potency with an IC_{50} of 10.45 μM, showing significant PARP1 inhibition. Docking analysis revealed strong and specific binding of **8e** to the PARP1 active site, supporting the experimental data.

Keywords: Breast cancer, PARP1, Thiouracil, Piperazine, Anticancer activity, Docking studies.

INTRODUCTION

Breast cancer remains one of the most prevalent and life-threatening malignancies affecting women across the globe, posing a significant challenge to public health systems [1]. Chemotherapeutic interventions serve as a cornerstone in its clinical management, primarily exerting their effects by suppressing the proliferation, invasion and metastatic dissemination of neoplastic cells. In contrast to normal somatic cells, malignant cells exhibit dysregulated cell-cycle control mechanisms, resulting in unchecked proliferation, accelerated metabolic activity and elevated levels of intrinsic oxidative and genotoxic stress [2,3]. Triple-negative breast cancers (TNBCs) represent an aggressive molecular subtype characterised by rapid tumor cell proliferation and are pathologically defined by the lack of estrogen receptor (ER), progesterone receptor (PR) and human epidermal growth factor receptor-2 (HER2) expression, which limit the therapeutic options available for targeted intervention [4-6].

Poly(ADP-ribose)polymerases (PARPs) constitute a multi-functional enzyme family responsible for catalyzing poly-(ADP-ribosyl)ation reactions that regulate a wide range of nuclear processes. Among the 17 members identified, PARP1 is the most abundant isoform and remains the most extensively characterised in terms of its structural and functional biology. These enzymes orchestrate key molecular events that govern chromatin remodelling, transcriptional regulation, DNA replication, homologous recombination and DNA damage repair mechanisms [7-9]. Structurally, PARP homologs contain conserved modular domains such as zinc finger motifs, BRCT (BRCA1 C-terminal), SAM (sterile alpha motif), SAP (SAF-A/B, Acinus, PIAS), ankyrin repeats and macro domains, each contributing to substrate recognition and enzymatic function [7-9]. Of these, PARP1 and PARP2 are the most biologically abundant and mechanistically elucidated members [7-9]. Upon DNA insult caused by exogenous agents including ionizing radiation, genotoxic chemicals or environmental stressors, PARP1 is promptly recruited to sites of DNA strand breaks

where it binds to damaged DNA segments [7,8,10,11]. Following activation, PARP1 catalyzes the transfer of ADP-ribose moieties from NAD^+ to itself and other nuclear proteins, generating extensive poly(ADP-ribose) (PAR) chains. This post-translational modification modulates chromatin accessibility and facilitates the recruitment of DNA repair machinery, thereby promoting the survival and persistence of cancer cells even under cytotoxic stress [12,13]. Recent preclinical findings indicate that PARP-DNA complex trapping elicits a more pronounced cytotoxic effect triggering apoptosis and replication fork collapse than inhibition of catalytic activity alone [12,13]. Pharmacologically, PARP inhibitors (PARPi) represent a class of targeted therapeutics that exploit synthetic lethality by preventing tumor cells deficient in homologous recombination repair from correcting DNA lesions. Approximately seventy small-molecule PARP inhibitors are currently under various stages of clinical evaluation, while olaparib, rucaparib, talazoparib and niraparib have gained FDA approval for clinical use [14-17].

Among the diverse chemical scaffolds explored for anticancer drug discovery, pyrimidine-based heterocycles have shown remarkable antineoplastic potential across multiple tumor models by interfering with critical oncogenic signaling cascades involved in cell cycle progression, angiogenesis and apoptosis regulation [9,18-20]. Notably, pyrimidine tethered piperazine derivatives have produced antiproliferative activity against MCF-7 cells by increasing the phosphorylation of H2A-X (histone family member X) and inhibited the catalytic activity of PARP [9]. We are actively contributing to synthetic organic chemistry [21-24] and medicinal chemistry by developing new anticancer agents [25-28]. Our continued efforts in this direction inspired to develop novel pyrimidine-piperazine hybrids as anticancer agents against MCF-7 breast cancer cells based on a previous report [9]. Furthermore, the mode of action of the designed molecules is identified through docking studies.

EXPERIMENTAL

All chemicals, reagents and solvents were procured from Sigma-Aldrich. ^1H and ^{13}C NMR spectra were measured in $CDCl_3$ as the solvent and TMS as the internal standard on Bruker WH-200 (400 MHz) and JEOL JSM-ECS (400 MHz) spectrometers. High-resolution mass spectra were obtained using Bruker Daltonics equipment. IR spectra were recorded using Perkin-Elmer spectrometer. Thin-layer chromatography (TLC) was performed to monitor the progress of the reactions.

General procedure for the synthesis of 2-(benzylthio)-6-methylpyrimidin-4-ols (3): A mixture of 6-methylthiouracil (**1**, 5.0 mmol), K_2CO_3 (6 mmol) and substituted benzyl chloride (6 mmol) in DMF (15 mL) was heated at 80 ºC. The reaction progress was monitored by TLC. Once the reaction was completed, the mixture was quenched using saturated sodium bicarbonate (25 mL) and subjected to extraction using ethyl acetate (50 mL × 2). Vacuum was applied to facilitate the formation of a concentrated product. Later crude product was purified through column chromatography on silica gel (60-120 mesh) using mixture of ethyl acetate and hexane (3:7).

General procedure for the synthesis of *tert*-butyl 2-((2-(benzylthio)-6-methylpyrimidin-4-yl)oxy)acetates (5): To a solution of **3** (4 mmol) in DMF (12 mL), K_2CO_3 (4.8 mmol) and *tert*-butyl bromoacetate (4.8 mmol) were added. This mixture was subjected to heating at 80 ºC subsequently reaction progress was observed recurrently using TLC. As soon as the reaction was completed, the reaction was quenched with saturated $NaHCO_3$ (25 mL), extracted with ethyl acetate (50 mL × 2) and subsequently subjected to the vacuum-mediated concentrated product. This crude product was later subjected to purification through column chromatography on silica gel (60-120 mesh) using mixture of ethyl acetate and hexane (3:7).

General procedure for the synthesis of 2-((2-(benzylthio)-6-methylpyrimidin-4-yl)oxy)acetic acids (6): Compound **5** (3 mmol) was dissolved in an aqueous THF (2:10; 10 mL) and stirred overnight with LiOH (3 mmol). TLC was used for monitoring the progression of the reaction. Upon completion, water (25 mL) was added and subsequently extracted using ethyl acetate (25 mL × 2). Later, vacuum was applied to generate the concentrated product (**Scheme-I**). Later, the final crude product was subjected to purification using column chromatography on silica gel (60-120 mesh), using mixture of ethyl acetate and hexane (5:5).

General procedure for the synthesis of pyrimidine-piperazine hybrids (8): Acid **6** (1.0 mmol) was reacted with piperazine derivative **7** (1.2 mmol) in the presence of 1-ethyl-3-(3-dimethylaminopropyl)carbodiimide hydrochloride (EDC·HCl, 1.2 mmol) and 4-dimethylaminopyridine (DMAP, 10 mol%) as a catalyst, using dichloromethane (DCM) as the solvent. To facilitate the coupling reaction, triethylamine (1.2 mmol) was added to the reaction mixture. The reaction was performed under a nitrogen atmosphere at room temperature. The progress of the reaction was monitored using thin-layer chromatography. Upon completion, the reaction was quenched by adding 10% sodium bicarbonate solution (25 mL). The reaction mixture was then extracted with ethyl acetate (25 mL × 2), which was subsequently concentrated under reduced pressure using a rotary evaporator (**Scheme-I**). The crude product was purified by column chromatography on silica gel (60-120 mesh) with a mixture of ethyl acetate and hexane (5:5) as mobile phase.

(2-((2-((4-Methoxybenzyl)thio)-6-methylpyrimidin-4-yl)oxy)-1-(4-(*p*-tolyl)piperazin-1-yl)ethan-1-one) (8a): Yield: 80%, white solid; m.p.: 138-141 ºC; IR (KBr, ν_{max}, cm^{-1}): 2833, 1668, 1443, 1030, 671; ^1H NMR (400 MHz, $CDCl_3$, δ ppm): 7.31 (d, *J* = 12.0 Hz, 2H), 7.1 (d, *J* = 8.0 Hz, 2H), 6.84-6.82 (m, 4H), 6.44 (s, 1H), 5.04 (s, 2H), 4.33 (s, 2H), 3.80 (s, 3H), 3.16-3.09 (m, 8H), 2.42 (s, 3H), 2.30 (s, 3H); ^{13}C NMR (100 MHz, $CDCl_3$, δ ppm): 169.96, 168.48, 168.25, 165.77, 160.74, 154.48, 133.61, 130.44, 115.42, 115.20, 102.63, 80.50, 63.17, 44.76, 41.82, 34.36, 28.40, 23.83, 22.99; HRMS (ESI) *m/z*: calcd. for $C_{26}H_{30}N_4O_3S$ $[M + H]^+$ 479.2117; found, 479.2119.

(1-(4-(4-Chlorophenyl)piperazin-1-yl)-2-((2-((4-methoxybenzyl)thio)-6-ethylpyrimidin-4-yl)oxy)ethan-1-one) (8b): Yield: 89%, off white solid; m.p.: 134-137 ºC; IR (KBr, ν_{max}, cm^{-1}): 2979, 1671, 1416, 1671, 1164, 724, 645; ^1H NMR (400 MHz, $CDCl_3$, δ ppm): 7.2 (d, *J* = 12.0 Hz, 2H), 7.08 (d, *J* = 5.0 Hz, 2H), 6.84-6.80 (m, 4H), 6.58 (s, 1H), 5.05 (s, 2H), 4.33 (s, 2H), 4.12 (s, 3H) 4,12 (s, 3H) 3.79 (s, 2H), 3.59 (s, 2H), 3.11 (d, *J* = 16.0 Hz, 4H), 2.29 (s, 3H); ^{13}C NMR (100

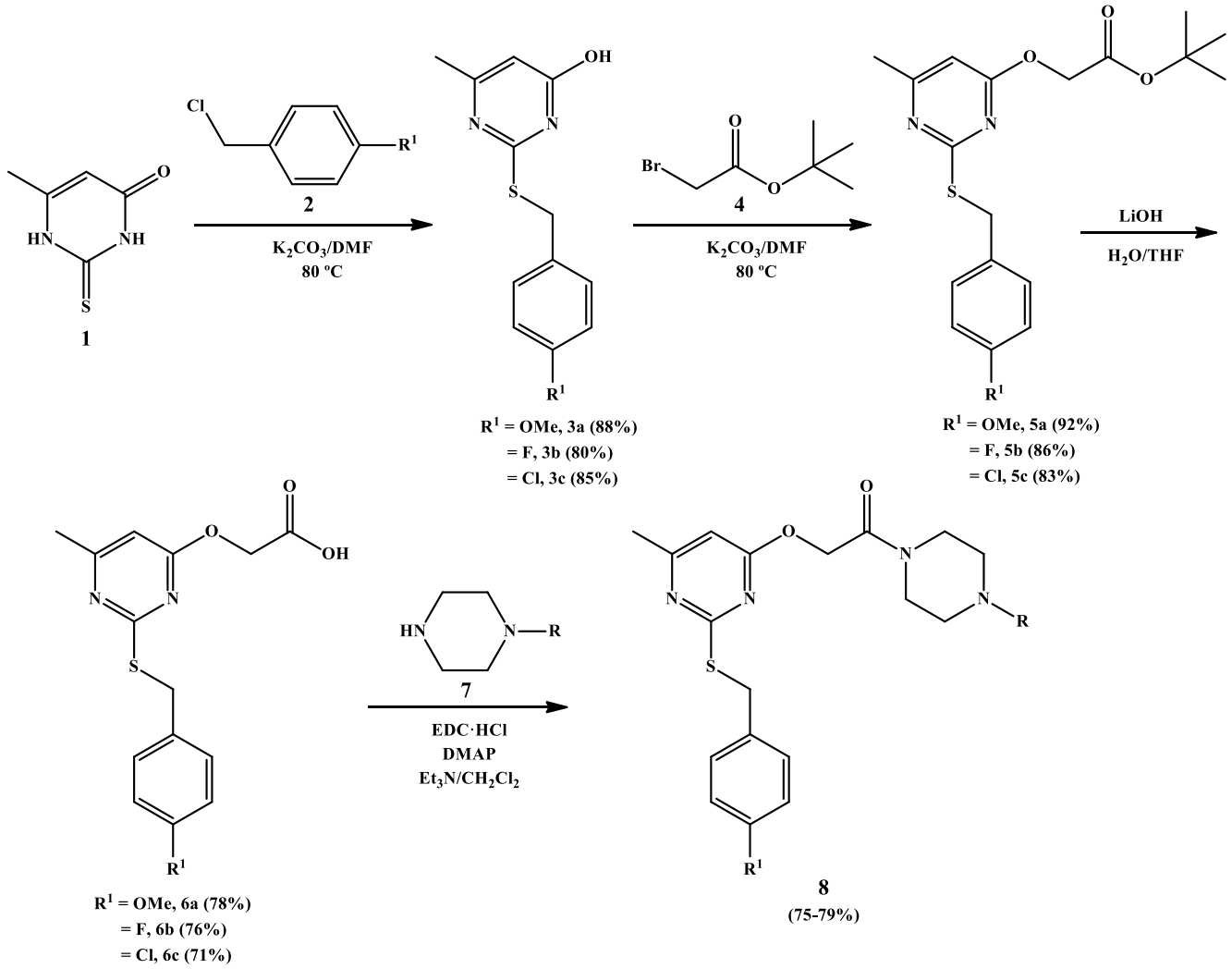

Scheme-I: Synthesis of pyrimidine-piperazine hybrids (**8a-j**)

MHz, $CDCl_3$, δ ppm): 169.96, 168.48, 168.25, 165.77, 160.74, 154.48, 133.61, 130.44, 115.42, 115.20, 102.63, 80.50, 63.17, 44.76, 41.82, 34.36, 28.40, 23.83; HRMS (ESI) *m/z*: calcd. for $C_{25}H_{27}ClN_4O_3S$ $[M + H]^+$ 499.1571; found, 499.1570.

(2-((2-((4-Methoxybenzyl)thio)-6-methylpyrimidin-4-yl)oxy)-1-(4-(4-nitrophenyl)piperazin-1-yl)ethan-1-one) (8c): Yield: 84%, orange solid; m.p.: 145-148 ºC; IR (KBr, ν_{max}, cm^{-1}): 2833, 1603, 1512, 1389, 1166, 671; ^1H NMR (400 MHz $CDCl_3$, δ ppm): 7.84-7.77 (m, 2H), 7.33 (d, *J* = 4.0 Hz, 2H), 7.06-7.03 (m, 2H), 6.85 (d, *J* = 8.5 Hz, 2H), 6.43 (s, 1H), 5.03 (s, 2H), 4.35 (s, 2H), 3.80 (s, 3H), 2.71 (s, 8H), 2.42 (s, 3H); ^{13}C NMR (100 MHz $CDCl_3$, δ ppm): 170.37, 168.45, 168.24, 165.70, 160.93, 158.81, 133.58, 133.46, 130.09, 125.91, 123.37, 121.87, 121.55, 120.94, 113.97, 102.51, 77.37, 77.05, 76.73, 63.05, 55.30, 51.64, 34.85, 23.84; HRMS (ESI) *m/z*: calcd. for $C_{25}H_{27}N_5O_5S$ $[M + H]^+$ 510.1811; found, 510.1814.

(1-(4-(2,3-Dichlorophenyl)piperazin-1-yl)-2-((2-((4-methoxybenzyl)thio)-6-methyl pyrimidin-4-yl)oxy)ethan-1-one) (8d): Yield: 85%, off white solid; m.p.: 140-143 ºC; IR (KBr, ν_{max}, cm^{-1}): 2861, 1669, 1392, 1237, 724; ^1H NMR (400 MHz $CDCl_3$, δ ppm): 7.40-7.36 (m, 3H), 7.29 (s, 1H), 7.02-6.97 (m, 3H), 4.98 (s, 2H), 4.34 (s, 2H), 3.46-3.42 (m, 12H), 2.41 (s, 3H); ^{13}C NMR (100 MHz, $CDCl_3$, δ ppm): 169.96, 168.48, 168.25, 165.77, 160.74, 154.48, 133.61, 130.44, 115.42, 115.20, 102.63, 80.50, 63.17, 44.76, 41.82, 34.36, 28.40, 23.83; HRMS (ESI) *m/z*: calcd. for $C_{25}H_{26}Cl_2N_4O_3S$ $[M + H]^+$ 533.1181; found, 533.1184.

(1-(4-(4-Chloro-2-fluorophenyl)piperazin-1-yl)-2-((2-((4-fluorobenzyl)thio)-6-methylpyrimidin-4-yl)oxy)-ethan-1-one (8e): Yield: 75%, white solid; m.p.: 135-140 ºC; IR (KBr, ν_{max}, cm^{-1}): 1666, 1390, 1166, 1034, 725, 648; ^1H NMR (400 MHz, $CDCl_3$, δ ppm): 7.40-6.83 (m, 7H), 6.45 (d, *J* = 8.0 Hz, 1H), 5.03 (s, 2H), 4.36 (s, 2H), 3.79 (s, 2H), 3.63-3.60 (m, 2H), 3.04-2.99 (m, 4H), 2.42 (s, 3H); ^{13}C NMR (100 MHz, $CDCl_3$, δ ppm): 169.93, 168.47, 168.33, 165.65, 163.20, 150.38, 134.20, 130.56, 130.48, 127.56, 125.38, 118.84, 115.46, 115.24, 102.68, 63.11, 45.13, 42.23, 34.49, 23.83; HRMS (ESI) *m/z*: calcd. for $C_{24}H_{23}ClF_2N_4O_2S$ $[M + H]^+$ 505.1277; found, 505.1275.

(1-(4-(2,3-Dichlorophenyl)piperazin-1-yl)-2-((2-((4-fluorobenzyl)thio)-6-ethylpyrimidin-4-yl)oxy)ethan-1-one) (8f): Yield: 78%, white solid; m.p.: 110-115 ºC; IR (KBr, ν_{max}, cm^{-1}): 1662, 1422, 1167, 1146, 723, 648; ^1H NMR (400 MHz, $CDCl_3$, δ ppm): 7.40-6.45 (m, 8H), 5.03 (s, 2H), 4.36

(s, 2H), 3.79 (s, 2H), 3.61 (d, *J* = 4.0 Hz, 2H), 3.05-2.98 (m, 4H), 1.77 (s, 3H); ^{13}C NMR (100 MHz, $CDCl_3$, δ ppm): 169.93, 168.37, 165.62, 163.22, 160.78, 150.39, 134.22, 133.47, 130.52, 127.55, 125.39, 118.84, 115.47, 115.25, 102.70, 63.15, 51.52, 51.02, 45.15, 42.24, 34.51, 23.78; HRMS (ESI) *m/z*: calcd. for $C_{24}H_{23}Cl_2FN_4O_2S$ $[M + H]^+$ 521.0981; found, 521.0983.

(*tert*-Butyl-4-(2-((2-((4-fluorobenzyl)thio)-6-methyl-pyrimidin-4-yl)oxy)acetyl)piperazine-1-carboxylate) (8g): Yield: 80%, white solid; m.p. 136-140 ºC; IR (KBr, ν_{max}, cm^{-1}): 1675, 1443, 1168, 1136, 726; ^{1}H NMR (400 MHz, $CDCl_3$, δ ppm): 7.40-7.36 (m, 2H), 7.02-6.97 (m, 2H), 6.43 (s, 1H), 4.34 (s, 2H), 3.58 (s, 2H), 3.58 (s, 2H)) 3.44 (d, *J* = 16.0 Hz, 7H), 2.41 (s, 3H), 1.48 (s, 9H); ^{13}C NMR (100 MHz, $CDCl_3$, δ ppm): 169.80, 168.49, 168.26, 165.64, 136.51, 132.90, 130.21, 128.57, 128.51, 102.67, 80.50, 63.19, 34.40, 34.30, 28.36, 23.82; HRMS (ESI) *m/z*: calcd. for $C_{23}H_{29}FN_4O_4S$ $[M + H]^+$ 477.1972; found, 477.1970.

(2-((2-((4-Fluorobenzyl)thio)-6-methyl pyrimidin-4-yl)-oxy)-1-(piperazin-1-yl)ethan-1-one) (8h): Yield: 75%, browish solid; m.p. 132-138 ºC; IR (KBr, ν_{max}, cm^{-1}): 1661, 1579, 1443, 1166, 1135, 723; ^{1}H NMR (400 MHz, $CDCl_3$, δ ppm): 7.35 (d, *J* = 8.0 Hz, 2H), 7.29-7.26 (m, 2H), 6.43 (s, 1H), 4.95 (s, 2H), 4.31 (d, *J* = 8.0 Hz, 3H), 3.64 (s, 2H), 3.47 (s, 2H), 3.04-2.91 (s, 3H), 2.40 (s, 3H); ^{13}C NMR (100 MHz, $CDCl_3$, δ ppm): 169.77, 168.58, 167.99, 165.57, 136.56, 132.88, 130.32, 129.59, 128.57, 102.70, 63.07, 45.07, 34.41, 23.81; HRMS (ESI) *m/z*: calcd. for $C_{18}H_{21}FN_4O_2S$ $[M + H]^+$ 377.1447; found, 377.1450.

(*tert*-Butyl4-(2-((2-((4-chlorobenzyl)thio)-6-methyl pyrimidin-4-l)oxy)acetyl)piperazine-1-carboxylate) (8i): Yield: 81%, white solid; m.p.: 110-115 ºC; IR (KBr, ν_{max}, cm^{-1}): 1601, 1444, 1165, 723, 646; ^{1}H NMR (400 MHz, $CDCl_3$, δ ppm): 7.52-7.20 (m, 4H), 6.42 (s, 1H), 4.96 (s, 2H), 4.32 (s, 2H), 3.56-3.35 (m, 8H), 2.40 (s, 3H), 1.47 (s, 9H), ^{13}C NMR (100 MHz, $CDCl_3$, δ ppm): 169.80, 168.49, 168.26, 165.75, 154.47, 136.51, 130.21, 128.57, 102.67, 80.50, 63.19, 44.74, 41.82, 34.40, 34.30, 28.36, 23.82; HRMS (ESI) *m/z*: calcd. for $C_{23}H_{29}ClN_4O_4S$ $[M + H]^+$ 493.1676; found, 493.1674.

(2-(2-((4-Chlorobenzyl)thio)-6-methylpyrimidin-4-yl)-oxy)-1-(piperazin-1-yl)ethan-1-one (8j): Yield: 84%, brownish solid; m.p.: 132-138 ºC; IR (KBr, ν_{max}, cm^{-1}): 1662, 1580, 1391, 1242, 723, 648; ^{1}H NMR (400 MHz, $CDCl_3$, δ ppm): 7.53-7.25 (m, 5H), 6.42 (s, 1H), 4.95 (s, 2H), 4.32 (s, 2H), 3.64 (s, 2H), 3.47 (s, 2H), 2.93 (d, *J* = 8.0 Hz 4H), 2.40 (s, 3H); ^{13}C NMR (100 MHz, $CDCl_3$, δ ppm): 169.77, 168.48, 168.29, 165.57, 136.56, 132.88, 130.25, 128.57, 102.70, 63.07, 45.26, 41.85, 34.41, 23.81; HRMS (ESI) *m/z*: calcd. for $C_{18}H_{21}ClN_4O_2S$ $[M + H]^+$ 393.1152; found, 393.1151.

Cell viability assay: Alamar blue was used for the cell viability experiment (Invitrogen, DAL1025, USA). In brief, 2×10^3 MCF-7 cells were seeded in 96-well plates and either the control medium (RPMI 1640; Gibco, 11875093, USA) supplemented with 2% FBS (cell-box, CF-01S-02, China) maintained at 37 ºC in a humidified 5% CO_2 incubator for 72 h or the compounds at 10-fold serial diluted concentrations (0.001, 0.01, 0.1, 1.0, 10.0 and 100.0 μM). Following treatment, the cells were placed in an incubator with 0.2 mL of 10% alamar blue solution at 37 ºC and 5% CO_2 for 4 h. They were subjected to rinsing with PBS. Next, using a Tecan microplate reader, fluorescence was assessed at an excitation wavelength of 575 nm and an emission wavelength of 595 nm. Dose-response curves were employed to assess IC_{50} values and the evaluated drugs were expressed as % of control cells. Using GraphPad Software 10.0 (GraphPad Inc., San Diego, CA, USA), the IC_{50} was computed for each experiment with determinations made in triplicate.

***In silico* analysis:** Molecular docking simulation was carried out using AutoDock4 tools [29]. Initially, the crystal structure of PARP1 (PDB ID: 4HHY) was obtained from Protein Data Bank. Protein structure was prepared by removing water molecules and heteroatoms to eliminate potential interference with docking results. Hydrogen atoms were subsequently added using BIOVIA Discovery Studio software, ensuring proper valence and saturation of the protein.

For ligand preparation, the three-dimensional structure of compound **8e** was generated and optimised using appropriate software to achieve a stable conformation. The known inhibitor of PARP1, talazoparib, was similarly generated and optimised. Both ligands were assigned partial charges to mimic physiological conditions accurately and saved in PDBQT format to ensure compatibility with AutoDock4 software.

Molecular docking simulations were then conducted using AutoDock4 tools. A grid box was typically prepared around the active site of PARP1 to accommodate both **8e** and talazoparib. The grid dimensions were set to 50 Å × 50 Å × 50 Å, with a grid spacing of 0.500 Å, providing a comprehensive exploration of the binding pocket. The Lamarckian Genetic Algorithm (LGA) was employed to search for favourable binding modes of **8e** and talazoparib within the active site of PARP1, taking into account both ligand flexibility and receptor conformational adjustments. The number of genetic algorithm runs was set to 10 to ensure robust sampling, while other parameters were maintained specifically at their default settings for consistency.

The docking results were visualised using Discovery Studio and UCSF Chimera [30], which facilitated the analysis of binding interactions, hydrogen bonds, hydrophobic contacts and conformational changes within the protein-ligand complexes. These visualisations provided insights into the binding affinity and potential efficacy of **8e** as a PARP1 inhibitor compared to the known inhibitor talazoparib.

RESULTS AND DISCUSSION

The title compounds pyrimidine-piperazine hybrids were synthesized according to **Scheme-I**. In brief, *S*-benzylation of 6-methylthiouracil **1** was initiated by using different benzyl chlorides **2** (R^1 = OMe, F, Cl) in the presence of K_2CO_3 in DMF at 80 ºC, to obtain 2-(benzylthio)-6-methylpyrimidin-4-ols **3a-c** in 80-88% yields. Later, O-alkylated **3** was done using *tert*-butyl bromoacetate **4** in the presence of K_2CO_3 in DMF at 80 ºC, which afforded *tert*-butyl 2-((2-(benzylthio)-6-methyl-pyrimidin-4-yl)oxy)acetates **5a-c** in 83-92% yields. In the next step, ester group of **5** was hydrolysed by using LiOH in aqueous THF, which results in the formation of 2-((2-(benzylthio)-6-methylpyrimidin-4-yl)oxy)acetic acids **6a-c** in 71-78% yields. Finally, acids **6** were coupled with diverse piperazine

derivatives **7** using EDC·HCl in the presence of triethylamine and catalytic amount of 4-*N*,*N*-dimethylaminopyridine (DMAP) in dichloromethane to get pyrimidine-piperazine hybrids **8** in 75-89% yields. In ^{1}H NMR spectra, all compounds exhibited a singlet around δ 2.5 ppm for methyl group on pyrimidine nucleus. Similarly, singlets were present for thiomethylene and oxymethylene groups around δ 4.4 and 5.0 ppm. Finally, due to the conformational asymmetry, piperazine hydrogens showed resonance between δ 3.00 and 3.10, δ 3.60 and 3.80 ppm.

Breast cancer cell viability: The synthesised pyrimidine-piperazine hybrids were evaluated for cell viability using the ER+ breast cancer cell line MCF-7 using alamar blue assay with tamoxifen and doxorubicin as internal standards and their IC_{50} values are given in Table-1. Based on the results, it was found that in the presence of methoxy group (R^1 = OMe), the order of anticancer activity was 4-NO_2 < 4-Me < 4-Cl (R). The 2,3-dichlorophenyl group was ineffective in this case. In the presence of fluoro group (R^1 = F), 2,3-dichlorophenyl-piperazine, *N*-Boc-piperazine and piperazine failed to induce good anticancer activity (>100 μM). Interestingly, 2-fluoro-4-chlorophenylpiperazine showed the highest activity (10.45 μM) against MCF-7. Finally, in the presence of chloro group, piperazine worked well (22.67 μM) than *N*-Boc-piperazine (>100 μM). The enhanced anticancer activity of the lead molecule **8e** is specifically due to interaction of fluorine at *o*-position with target enzyme.

TABLE-1
In vitro IC_{50} VALUES (μM) AND PREDICTED BINDING ENERGIES (kcal/mol) OBTAINED FROM MOLECULAR DOCKING STUDIES FOR PYRIMIDINE–PIPERAZINE HYBRID DERIVATIVES (**8a-j**)

Compd.	R^1	R	IC_{50} (μM)	Binding energy (kcal/mol)
8a	OMe	4-MeC_6H_4	69.98	-8.91
8b	OMe	4-ClC_6H_4	48.00	-8.96
8c	OMe	4-$NO_2C_6H_4$	>100	-8.46
8d	OMe	2,3-$Cl_2C_4H_3$	>100	-8.51
8e	F	2-F-4-ClC_4H_3	10.45	-9.12
8f	F	2,3-$Cl_2C_4H_3$	>100	-8.63
8g	F	Boc	>100	-8.18
8h	F	H	>100	-8.62
8i	Cl	Boc	22.67	-9.00
8j	Cl	H	>100	-8.83

IC_{50} values of tamoxifen and doxorubicin were 1.75 and 0.73 μM, respectively.

***In silico* analysis:** Present study focuses on the *in silico* analysis of a newly synthesised compound **8e** designed to target the active site of PARP1 and to evaluate its potential as a PARP1 inhibitor (Fig. 1). The binding energy was compared with that of the standard PARP1 inhibitor talazoparib using molecular docking simulations. The molecular docking results revealed that **8e** exhibited a binding energy of -9.12 kcal/mol (Table-1), where hydrogen bond formed with ARG-204 with distance of 2.22 Å, π-anion bonds formed with ASP-109 and ASN-207 with distances of 4.00 Å and 5.12 Å. A halogen (fluorine) bonded with GLY-202 and ARG-217 with bond distances 2.57 Å and 2.74 Å respectively, Π-sulfur

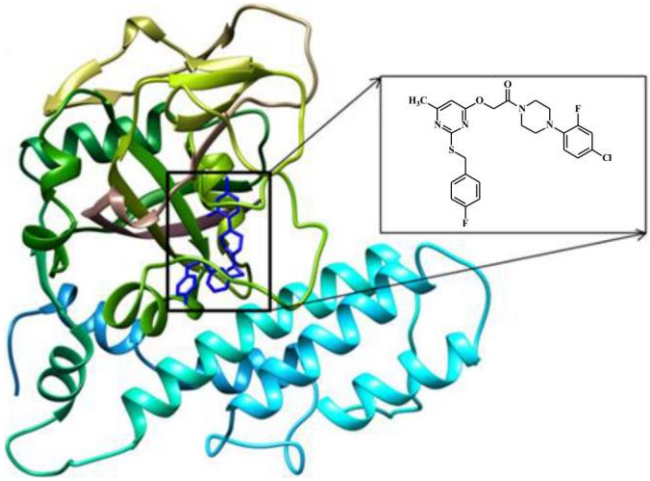

Fig. 1. Cartoon representation of compound **8e** docked within the active site of PARP1

bond formed with HIS-201 and further hydrophobic interactions (π-π stacked and π-alkyl) were observed with TYR-246 and ILE-211 (Fig. 2a). While, talazoparib demonstrated a slightly higher binding energy of -9.29 kcal/mol where hydrogen bonds formed with GLY-202 and SER-243 with bond distance of 2.32Å and 1.92 Å, respectively. A halogen (fluorine) bond formed with PHE-236 and hydrophobic interactions (π-π stacked, π-π T-shaped, π-alkyl) with TYR-246, HIS-201, GLY-227, TYR-235, PHE-236, ALA-237 and LYS-242 were also observed (Fig. 2b). The comparative analysis suggested that the binding energy of **8e** is comparable to that of the standard inhibitor talazoparib, indicating its potential as a PARP1 inhibitor. Therefore, the *in silico* analysis of **8e** targeting the active site of PARP1 demonstrated promising binding affinity, comparable to the standard inhibitor talazoparib (Fig. 3). These findings provide a basis for further experimental validation and optimisation of **8e** as a potential PARP1 inhibitor for breast cancer therapy. The binding energies of rest of the molecules are presented in Table-1, which indicated that active compounds exhibited high binding energies than inactive compounds (>100 μM).

Conclusion

In summary, novel pyrimidine-piperazine hybrids were synthesised and identified as potential PARP inhibitors. The Alamar blue assay further revealed that compound **8e** had an IC_{50} of 10.45 μM, indicating significant cytotoxicity against MCF-7 cancer cells. A comparison with the reported synthetic compounds indicated that structurally variations in the present study significantly influenced the anticancer activity of the molecules, which act as PARP inhibitors. The newly synthesised **8e** derivative exhibited more anticancer activity against the MCF-7 breast cancer cell line, with an IC_{50} value of 10 μM. The *in silico* analysis outlined that **8e** could effectively inhibit PARP1 in MCF-7 cells.

ACKNOWLEDGEMENTS

This work was supported by the Vision Group on Science and Technology (CESEM) and the Government of Karnataka.

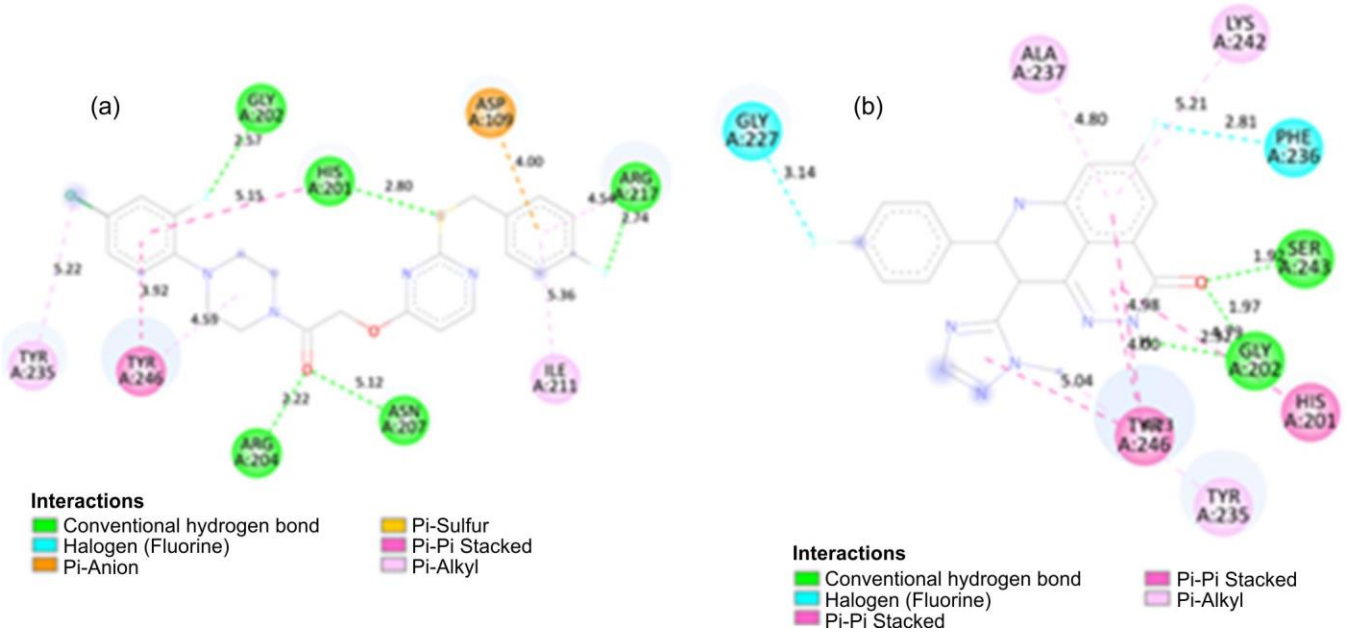

Fig. 2. (a) 2D structure of compound **8e** depicting specific interactions with amino acid residues of PARP1 and (b) comparison of 2D structure of **8e** with talazoparib

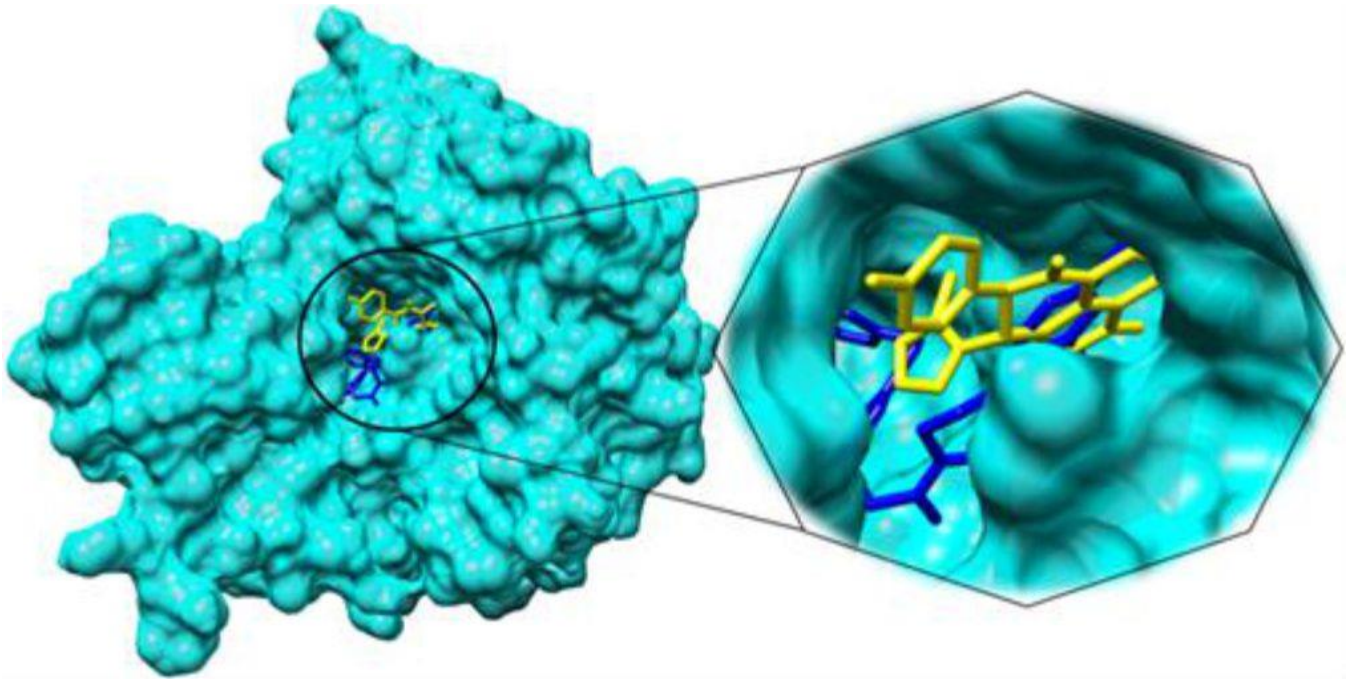

Fig. 3. 3D surface view of docked compounds **8e** (blue) and talazoparib (yellow) within the PARP1 active site. The enlarged view provides a detailed visualisation of their binding orientations and interactions, aiding in understanding their binding affinities and potential inhibitory mechanisms

CONFLICT OF INTEREST

The authors declare that there is no conflict of interests regarding the publication of this article.

DECLARATION OF AI-ASSISTED TECHNOLOGIES

During the preparation of this manuscript, the authors used an AI-assisted tool(s) to improve the language. The authors reviewed and edited the content and take full responsibility for the published work.

REFERENCES

1. R.L. Siegel, K.D. Miller and A. Jemal, *CA Cancer J. Clin.*, **69**, 7 (2019); https://doi.org/10.3322/caac.21551.
2. H. Yao, G. He, S. Yan, C. Chen, L. Song, T.J. Rosol and X. Deng, *Oncotarget*, **8**, 1913 (2017); https://doi.org/10.18632/oncotarget.12284

3. P.M. Uppar, N.Y. Kim, K.K. Harish, N.M. Beeraka, S.L. Gaonkar, M. Madegowda, K.S. Rangappa, V.N. Nikolenko, A. Chinnathambi, G. Sethi, S.A. Alharbi, K.S. Ahn and B. Basappa, *Chem. Biol. Interact.*, **415**, 111528 (2025); https://doi.org/10.1016/j.cbi.2025.111528
4. K. Basappa Sugahara, K.N. Thimmaiah, H.K. Bid, P.J. Houghton and K.S. Rangappa, *PLoS One*, **7**, e39444 (2012); https://doi.org/10.1371/journal.pone.0039444
5. L. Yin, J.-J. Duan, X.-W. Bian and S.-C. Yu, *Breast Cancer Res.*, **22**, 61 (2020); https://doi.org/10.1186/s13058-020-01296-5
6. J. Pang, N. Ding, X. Liu, X. He, W. Zhou, H. Xie, J. Feng, Y. Li, Y. He, S. Wang and Z. Xiao, *Ann. Surg. Oncol.*, **32**, 750 (2025); https://doi.org/10.1245/s10434-024-16454-8
7. P. Jagtap and C. Szabó, *Nat. Rev. Drug Discov.*, **4**, 421 (2005); https://doi.org/10.1038/nrd1718
8. F. Mégnin-Chanet, M.A. Bollet and J. Hall, *Cell. Mol. Life Sci.*, **67**, 3649 (2010); https://doi.org/10.1007/s00018-010-0490-8
9. S.N. Deveshegowda, P.K. Metri, R. Shivakumar, J.-R. Yang, S. Rangappa, A. Swamynayaka, M.K. Shanmugam, O. Nagaraja, M. Madegowda, P. Babu Shubha, A. Chinnathambi, S.A. Alharbi, V. Pandey, K.S. Ahn, P.E. Lobie and B. Basappa, *Molecules*, **27**, 2848 (2022); https://doi.org/10.3390/molecules27092848
10. Y. Wang, W. Luo and Y. Wang, *DNA Repair*, **81**, 102651 (2019); https://doi.org/10.1016/j.dnarep.2019.102651
11. E.E. Alemasova and O.I. Lavrik, *Nucleic Acids Res.*, **47**, 3811 (2019); https://doi.org/10.1093/nar/gkz120
12. D.K. Nambiar, D. Mishra and R.P. Singh, *Oncol. Res.*, **31**, 405 (2023); https://doi.org/10.32604/or.2023.028310
13. H.L. Ko and E.C. Ren, *Biomolecules*, **2**, 524 (2012); https://doi.org/10.3390/biom2040524
14. T.A. Hopkins, Y. Shi, L.E. Rodriguez, L.R. Solomon, C.K. Donawho, E.L. DiGiammarino, S.C. Panchal, J.L. Wilsbacher, W. Gao, A.M. Olson, D.F. Stolarik, D.J. Osterling, E.F. Johnson and D. Maag, *Mol. Cancer Res.*, **13**, 1465 (2015); https://doi.org/10.1158/1541-7786.MCR-15-0191-T
15. G. Barchiesi, M. Roberto, M. Verrico, P. Vici, S. Tomao and F. Tomao, *Front. Oncol.*, **11**, 769280 (2021); https://doi.org/10.3389/fonc.2021.769280
16. L. Cortesi, H.S. Rugo and C. Jackisch, *Target. Oncol.*, **16**, 255 (2021); https://doi.org/10.1007/s11523-021-00796-4
17. M.A. Bruin, G.S. Sonke, J.H. Beijnen and A.D. Huitema, *Clin. Pharmacokinet.*, **61**, 1649 (2022); https://doi.org/10.1007/s40262-022-01167-6
18. B. Tylińska, B. Wiatrak, Z. Czyżnikowska, A. Cieśla-Niechwiadowicz, E. Gębarowska and A. Janicka-Kłos, *Int. J. Mol. Sci.*, **22**, 3825 (2021); https://doi.org/10.3390/ijms22083825
19. N.Y. Kim, D. Vishwanath, Z. Xi, O. Nagaraja, A. Swamynayaka, K. Kumar Harish, S. Basappa, M. Madegowda, V. Pandey, G. Sethi, P.E. Lobie, K.S. Ahn and B. Basappa, *Molecules*, **28**, 3450 (2023); https://doi.org/10.3390/molecules28083450
20. A. Ravish, B.C. Narasimhachar, Z. Xi, D. Vishwanath, A. Mohan, S.L. Gaonkar, P.G. Chandrashekara, K.S. Ahn, V. Pandey, P.E. Lobie and B. Basappa, *Biomedicines*, **11**, 2716 (2023); https://doi.org/10.3390/biomedicines11102716
21. T.R. Swaroop, Z.-Q. Wang, Q.Y. Li and H.-S. Wang, *J. Electrochem. Soc.*, **167**, 046504 (2020); https://doi.org/10.1149/1945-7111/ab72ed
22. N. Rajeev, T.R. Swaroop, S.M. Anil, K.R. Kiran, K.S. Rangappa and M.P. Sadashiva, *J. Chem. Sci.*, **130**, 150 (2018); https://doi.org/10.1007/s12039-018-1540-2
23. C. Santhosh, K.R. Singh, K. Sheela, T.R. Swaroop and M.P. Sadashiva, *J. Org. Chem.*, **88**, 11486 (2023); https://doi.org/10.1021/acs.joc.3c00589
24. K.R. Kiran, T.R. Swaroop, C. Santhosh, K.S. Rangappa and M.P. Sadashiva, *ChemistrySelect*, **6**, 7262 (2021); https://doi.org/10.1002/slct.202102071
25. S.D. Preethi, K.S. Balaji, D.S. Prasanna, T.R. Swaroop, J. Shankar, K.S. Rangappa and S. Lokesh, *Anticancer. Agents Med. Chem.*, **17**, 1931 (2017).
26. R. Roopashree, C.D. Mohan, T.R. Swaroop, S. Jagadish and K.S. Rangappa, *Asian J. Pharm. Clin. Res.*, **7**, 309 (2014).
27. Dukanya, T.R. Swaroop, K.S. Rangappa and Basappa, *Curr. Org. Chem.*, **24**, 2792 (2020); https://doi.org/10.2174/1385272824999201020204001
28. S.M. Anil, M.S. Sudhanva, T.R. Swaroop, A.C. Vinayaka, N. Rajeev, K.R. Kiran, R. Shobith and M.P. Sadashiva, *Chem. Biodivers.*, **17**, e2000014 (2020); https://doi.org/10.1002/cbdv.202000014
29. R. Huey, G.M. Morris, A.J. Olson and D.S. Goodsell, *J. Comput. Chem.*, **28**, 1145 (2007); https://doi.org/10.1002/jcc.20634
30. E.F. Pettersen, T.D. Goddard, C.C. Huang, G.S. Couch, D.M. Greenblatt, E.C. Meng and T.E. Ferrin, *J. Comput. Chem.*, **25**, 1605 (2004); https://doi.org/10.1002/jcc.20084